HHS Public Access

Author manuscript

J Biomed Mater Res A. Author manuscript; available in PMC 2019 June 15.

Published in final edited form as:

J Biomed Mater Res A. 2018 February ; 106(2): 500–509. doi:10.1002/jbm.a.36245.

Multimodal pore formation in calcium phosphate cements

Irene Lodoso-Torrecilla[1], **Nicole A. P. van Gestel**[2,3], **Luis Diaz-Gomez**[4,5], **Eline-Claire Grosfeld**[1], **Kjell Laperre**[6], **Joop G. C. Wolke**[1], **Brandon T. Smith**[5], **Jacobus J. Arts**[2,7], **Antonios G. Mikos**[5,8], **John A. Jansen**[1], **Sandra Hofmann**[2,3,9], and **Jeroen J. J. P. van den Beucken**[1]

[1]Department of Biomaterials, Radboudumc, Nijmegen, The Netherlands [2]Orthopedic Biomechanics, Department of Biomedical Engineering, Eindhoven University of Technology, Eindhoven, The Netherlands [3]Institute for Complex Molecular Systems, Eindhoven University of Technology, Eindhoven, The Netherlands [4]Departamento de Farmacia y Tecnología Farmacéutica, Facultad de Farmacia, Universidade de Santiago de Compostela, Santiago de Compostela, Spain [5]Department of Bioengineering, Rice University, Houston, Texas 77030 [6]Bruker microCT, Kontich, Belgium [7]Department of Orthopaedic Surgery, Research School CAPHRI, Maastricht University Medical Centre, Maastricht, The Netherlands [8]Department of Chemical and Biomolecular Engineering, Rice University, Houston, Texas 77005 [9]Institute for Biomechanics, Swiss Federal Institute of Technology Zürich (ETHZ), Zürich, Switzerland

Abstract

Calcium phosphate cements (CPCs) are commonly used as bone substitute materials. However, their slow degradation rate and lack of macroporosity hinders new bone formation. Poly($_{DL}$-lactic-*co*-glycolic acid) (PLGA) incorporation is of great interest as, upon degradation, produces acidic by-products that enhance CPC degradation. Yet, new bone formation is delayed until PLGA degradation occurs a few weeks after implantation. Therefore, the aim of this study was to accelerate the early stage pore formation within CPCs *in vitro*. With that purpose, we incorporated the water-soluble porogen sucrose at different weight percentages (10 or 20 wt %) to CPC and CPC/PLGA composites. The results revealed that incorporation of sucrose porogens increased mass loss within the first week of *in vitro* degradation in groups containing sucrose compared to control groups. After week 1, a further mass loss was observed related to PLGA and CPC degradation. Macroporosity analysis confirmed that macroporosity formation is influenced by the dissolution of sucrose at an early stage and by the degradation of PLGA and CPC at a later stage. We concluded that the combination of sucrose and PLGA porogens in CPC is a promising approach to promote early stage bone tissue ingrowth and complete replacement of CPC through multimodal pore formation.

Keywords

calcium phosphate cement; PLGA; sucrose; degradation; porosity

Correspondence to: J. J. J. P. van den Beucken; jeroen.vandenbeucken@radboudumc.nl.

INTRODUCTION

Calcium phosphate (CaP) ceramics are being widely used as off-the-shelf alternatives to autologous bone grafts in multiple bone regeneration and augmentation procedures due to their similar composition to the native bone mineral, biocompatibility, and bioactivity.[1–3] CaP ceramics are available in different shapes, such as granules, blocks and cements. Of those, calcium phosphate cements (CPCs) are particularly appealing, as these are injectable pastes that can harden *in situ,* enabling minimally invasive surgeries.[4] Beside injectability, the biological properties (i.e., biocompatibility, osteoconductivity, and bioactivity) of CPCs make that they can be integrated within the bone tissue by similar processes as those involved in remodeling healthy bone.[5–7] CPCs can be roughly divided in two categories depending on the end-product of the reaction between the powder and liquid phase: apatite or brushite. Apatitic CPCs are more similar to the mineral phase of bone and their mechanical properties are superior to brushite CPCs.[8,9] Consequently, most research has focused on apatitic CPCs. However, apatitic CPCs degrade at a slow rate *in vivo*, which hinders full bone regeneration, as only limited space becomes available for new bone formation.[5,10,11] It is known that the presence of macroporosity is beneficial for CPC degradation and new bone formation, since the macroporosity allows fluid inflow as well as cell migration into the cement.[12]

Several approaches have been explored to enhance macroporosity within CPCs. For instance, foaming agents such as hydrogen peroxide or carbon dioxide have been used to create macroporosity within CPCs.[4,12–14] However, the pore size distribution appeared difficult to control and these agents are potentially harmful when used *in situ*. Another widely studied method is the introduction of polymeric porogens. Among the different polymers that have been used, poly($_{DL}$-lactic-*co*-glycolic acid) (PLGA) has shown to be particularly effective for this purpose. PLGA degrades by hydrolysis of its ester groups, which results in the creation of macroporosity in the ceramic CPC matrix and the release of the acidic monomers (i.e., lactic and glycolic acid) of PLGA. These monomers decrease the pH locally, which accelerates CPC degradation.[15,16] PLGA degradation is influenced by different factors, including the lactic to glycolic ratio and the polymer chain length.[17] Félix Lanao et al.[16,18] studied the effect of multiple PLGA porogen characteristics (i.e., molecular weight, porogen morphology [hollow vs. dense] and end-group functionalization) on *in vitro* and *in vivo* CPC degradation and found that both PLGA morphology and end-group functionalization had a strong influence on CPC degradation and macroporosity formation. Further studies investigated the effect of PLGA particle size on CPC degradation and demonstrated that size is important for hollow PLGA porogens, but not for dense PLGA.[19,20] Grosfeld et al.[21] recently showed that bone regeneration using CPC/PLGA is delayed compared to the dental predicate device Bio-Oss, because PLGA degradation only starts after approximately 2 weeks.

To rapidly obtain macroporosity, water-soluble porogens such as carbohydrates or salts seem appealing,[22–26] as after CPC injection into a bone defect, these porogens rapidly dissolve and generate macroporosity in the CPC matrix. However, the fast dissolution of such porogens also represents an issue, as their dissolution might already occur during or even before CPC setting. To overcome this problem, various measures can be taken: the liquid

phase can be saturated for the dissolved porogen, or kept at low temperatures, or the porogen can be used in frozen state or under liquid nitrogen conditions to prevent dissolution.[25,26] A disadvantage of carbohydrates and salts for the use as porogens is that except for a passive role in CPC degradation (i.e., by enlarging the CPC surface area available for interaction with the biological surrounding), these porogens do not play an active role to aid in CPC degradation (e.g., by acidic degradation products that degrade the CPC matrix).

The aim of this study was to evaluate multimodal pore formation behavior and degradation of CPC upon the incorporation of sucrose or PLGA porogens, or a combination thereof. We hypothesized that sucrose porogens can provide early pore formation upon rapid dissolution, whereas PLGA porogens can provide late pore formation and accelerate CPC degradation upon hydrolytic degradation and the acidic nature of its degradation products. For this, we explored handling properties and performed *in vitro* degradation experiments combined with mercury porosimetry, helium pycnometry and microcomputed tomography (microCT) to analyze pore formation behavior.

MATERIALS AND METHODS

Materials

CPC powder consisted of 100% alpha tricalcium phosphate (α-TCP) (CAM Bioceramics BV; Leiden, The Netherlands). Sodium dihydrogen phosphate dihydrate (NaH_2PO_4) was purchased from Merck (Darmstadt, Germany) and used as the liquid phase for the cement preparation. PLGA (lactic:-glycolic acid ratio 50:50; molecular weight of 17 kDa; acid-terminated) was used (Corbion Purac, Gorinchem, The Netherlands) in the form of microparticles (mean particle size of approximately 60 μm). Sucrose was purchased from Merck (mean particle size of approximately 400 μm).

Preparation of the CPC formulations

Sucrose and/or PLGA particles were added to α-TCP powder in different ratios (Table I). The amount of liquid phase (liquid-to-powder ratio [LPR]) was optimized to obtain cement formulations that exhibited comparable consistency (Table I). An 8 wt/vol % aqueous solution of NaH_2PO_4 was used at 4°C in order to prevent rapid sucrose dissolution. After combining the α-TCP with sucrose and/or PLGA porogens with the liquid phase, the mixture was mixed for 20 s with a spatula and the paste was inserted into polytetrafluorethylene mold (cylinder shaped, diameter = 4.5 mm, height = 9 mm) to obtain samples of similar dimensions. Subsequently, the samples were left overnight at room temperature to allow for hardening and were freeze dried to eliminate residual liquid.

Setting time measurement

The initial and final setting time of the various CPC formulations was assessed using Gillmore needles (ASTM C266). Briefly, a bronze block was used as mold containing holes of 6 mm diameter and 12 mm height. The mold was placed in a water bath at 37°C. Powder and liquid components of each CPC formulation were mixed and the resulting paste was placed into the mold. The Gillmore needles were lowered onto the cement and the initial and

final setting time were recorded when penetration was not observed anymore. Tests were performed in triplicate ($n = 3$).

Injectability analysis

The injectability of the different formulations was assessed by measuring the mass of CPC extruded from a 2.5 mL syringe with a nozzle orifice of 2 mm in diameter (Terumo Europe N.V., Leuven, Belgium) relative to the original mass of only the CPC paste [Eq. (1)].[27] The injection time was kept at 1:30 min in order to avoid that the initial setting time of the cement had an influence on the results. Tests were performed in triplicate ($n = 3$).

$$\% \text{ injectability} = \frac{m_n}{m_i} \times 100\% \quad (1)$$

where m_n is the mass of CPC remaining in syringe after injection (g) and m_i the mass of CPC before injection (g).

Washout of the cements

For determination of the cohesive properties of the different formulations, a washout test was performed as a quantitative analysis to measure the weight loss of CPCs upon immersion in phosphate-buffered saline (PBS; Gibco ®, Thermo Scientific, Waltham, MA) related to the calcium phosphate particles fragmented off of the sample and washed away. Briefly, the different CPC compositions were mixed with the liquid phase and the pastes were placed in tissue specimen bags (pore size = 170 μm; Thermo Scientific). Subsequently, the tissue bags were immersed in Falcon tubes containing 15 mL of PBS and immediately placed on a shaking table (120 rpm) inside an incubator at 37°C. After 4 h, both the tissue bags and the tubes were freeze-dried at −50°C until complete drying. The weight of both the CPC remaining in the bag (W_{CPC}) and the washed-out particles in the tube (W_{washed}) were measured and the wash out % was calculated using Eq. (2). Tests were performed in triplicate ($n = 3$).

$$\% \text{ washed} = \frac{W_{washed}}{W_{washed} + W_{CPC}} \times 100\% \quad (2)$$

In vitro degradation studies

For the degradation studies, each CPC sample was incubated in 10 mL of PBS (pH 7.4) at 37°C for 1 and 7 days to observe short term degradation behavior and for 1, 2, 4 and 6 weeks to evaluate long term degradation behavior. At each time point, four specimens of each CPC formulation were subjected to analysis. Directly after removal of the samples from the PBS, the pH was measured using a pH electrode (Orion, Sigma Aldrich) as a quantification of PLGA degradation. In order to quantify mass loss, samples were freeze-dried overnight. The remaining material of the samples was calculated using Eq. (3).

$$\%\ \text{Remaining material} = \frac{m_i - m_n}{m_i} \times 100\% \quad (3)$$

where m_n is the mass of the sample at $t = n$ (g) and m_i is the mass of the sample at $t = 0$ (g).

For sucrose and calcium release quantification, three specimens of each CPC formulation were incubated in 10 mL of PBS at 37°C for 6 weeks. At 1, 2, 4 and 6 weeks 0.5 mL of PBS were retrieved for analysis and were replaced by 0.5 mL of fresh PBS to keep the PBS volume constant. A calcium assay was performed to assess the amount of calcium released from the cement as a sign of CPC degradation. Sucrose in retrieved PBS was quantified by the phenol sulfuric method.[28] Briefly, 120 μL of PBS were pipetted into a 0.75 mL Eppendorf and 60 μL of 5% phenol were added. Then 300 μL of concentrated sulfuric acid (99.9%) were added rapidly for thorough mixing. The tubes were allowed to stand 10 min, then they were shaken in a vortex for 10 s and 200 μL of solution from each Eppendorf were pipetted into a 96-well plate, which was placed for 10–20 min in a water bath at 25°C before measuring absorbance at 490 nm.

The morphology of the CPCs was evaluated by scanning electron microscopy (SEM, Zeiss Sigma 300) before incubation in PBS (week 0) and after 1 and 6 weeks of incubation. Prior to SEM examination, samples were sputter coated with gold. Images were taken at an accelerating voltage of 3 kV under high vacuum.

Porosity evaluation

Total porosity, open porosity and macroporosity of the different cement formulations were determined by different methods. Total porosity (%) before degradation (week 0) and at week 1 and 6 of degradation was calculated from the skeletal and apparent densities [Eq. (4)]. The skeletal density (ρ_{skel}) of the scaffolds was calculated from ten replicates by gas displacement measurement using a helium pycnometer (Quantachrome, FL) at operating conditions of 25°C and 1.03 bar (1.02 atm) and a resolution of 1 Å. The apparent density (ρ_{app}) was determined from the measured weight and dimension of the samples after 1 and 6 weeks of degradation.

$$\text{Total porosity}\ (\%) = \left(1 - \frac{\rho_{app}}{\rho_{skel}}\right) \times 100\% \quad (4)$$

Open porosity at week 1 and 6 of degradation was determined by mercury intrusion porosimetry using a Micromeritics 9305 pore sizer (Micromeritics Instrument Corp., GA) with a resolution of 3 nm. Working pressures ranged between 0.07 and 1723 bars.

MicroCT (Skyscan 1275, Bruker MicroCT, Belgium) was performed to observe the macroporosity and pore formation behavior of the composites as a function of *in vitro* degradation at 0, 1, 2, 4 and 6 weeks. Tomographs were recorded at a voltage of 70 kV and a

current of 140 mA. The scanning resolution was set to 7 μm at a rotation step of 0.6°. Images were reconstructed using NRecon Reconstruction (Bruker MicroCT) and the macroporosity and pore size distribution were quantified with CTAn (Bruker MicroCT) using a 3.8 mm diameter × 2.1 mm height cylindrical volume of interest (VOI) to eliminate edge effects. For porosity analysis, each VOI was binarized using a global threshold of 35–255.

A CPC/PLGA/S20 sample was subjected to microCT analysis to study pore formation and degradation behavior. The sample was fixed in a custom-made bioreactor for longitudinal monitoring, adapted from Hagenmüller et al.[29] With this bioreactor, the degradation of each sample could be followed nondestructively over time. MicroCT images (μCT80, Scanco Medical AG, Brüttisellen, Switzerland) were obtained after 0, 1, 2, 4 and 6 weeks of soaking in 10 mL PBS. For the measurement, the following settings were chosen: an isotropic voxel size of 18 μm; a peak energy of 45 kVp; a current of 88 μA; and an integration time of 300 ms. Image analysis of the obtained scans was performed with the software IPLFE v02.01 (Scanco Medical, Brüttisellen, Switzerland). An algorithm for automatic edge detection was used to define the contours of the raw images at the edges of the CPC/PLGA/S20 sample. This algorithm makes use of predefined segmentation thresholds, which are based on the attenuation coefficients of the scanned sample. In the current study, a threshold of 356.4–1498 mg HA/ccm was defined for the samples, determined from the histogram of attenuation coefficients in the images. The determined contours were then used to register the images obtained at $t = 0$ (image 1) and at $t \neq 0$ (image 2), using a registration algorithm that minimizes the differences between two images by translations and rotations. The addition of the transformed image 2 to image 1 was used to determine the amount of degraded material being material that was present only at $t = 0$.[30] The image was color coded for visualization of degrading material and the degraded volume was quantified by summarizing the degraded voxels.

Statistical analysis

Statistical analysis was performed using Graphpad Prism 5 (GraphPad Software Inc., San Diego, CA). Significant differences between groups were determined using analysis of variance with Tukey's multiple comparison tests. Results were considered significant at p values lower than 0.05 ($p < 0.05$).

RESULTS

Handling properties

Setting time measurements (Table II) showed similar initial setting times (3.1–4.1 min) for all cement formulations, except for the formulations containing 20 wt % of sucrose. On the other hand, final setting times varied from 7.4 min for plain CPC to up to 80 min for CPC/PLGA/S20. Both the addition of PLGA and sucrose negatively affected final setting time.

Figure 1(a) reveals that the injectability increased with increasing amounts of sucrose porogen up to ~80% in the groups containing 20 wt % of sucrose. Addition of PLGA porogens, on the other hand, did not have a significant effect on injectability ($p > 0.05$).

Washout of the different formulations [Fig. 1(b)] showed that the addition of PLGA porogens did not significantly affect the washout properties of the cement formulations. The addition of sucrose porogens did not affect washout properties at 10 wt %, but washout increased to approximately 30–36% for 20 wt %.

In vitro degradation studies

In vitro degradation of pre-set CPC samples was assessed using mass loss measurements (Fig. 2). Samples containing sucrose porogens reduced their mass within 1 week to 93.8 ± 1.1, 85.5 ± 0.9, 94.8 ± 5.3 and 89.3 ± 1.5% for CPC/ S10, CPC/S20, CPC/PLGA/S10 and CPC/PLGA/S20, respectively [Fig. 2(b)]. On the other hand, the mass of CPC and CPC/PLGA remained stable during the first week. Samples containing different amounts of sucrose porogens (that is, 0, 10, and 20 wt %) had significantly different mass loss ($p < 0.01$), while the presence of PLGA did not affect the mass loss during week 1. After week 1, samples containing PLGA porogens started degrading to a further extent, and at week 6 only 48.7 ± 2.1, 44.0 ± 2.5, and 38.6 ± 0.9% of the material was remaining for CPC/PLGA, CPC/PLGA/S10, and CPC/PLGA/S20, respectively.

The pH measurements are shown in Fig. 2(c). During the first week, a marginal pH decrease was observed for all groups. After the first week, PLGA-containing samples showed a fast acidification that stabilized after 4 weeks at a pH of approximately 3.9. This pH was significantly lower ($p < 0.001$) than for CPC samples without PLGA, where pH values after 6 weeks were approximately 6.3.

CPC matrix degradation was determined by calcium release measurements in the incubation media [Fig. 2(d)]. For CPC, CPC/S10 and CPC/S20 this release was limited. After 1 week these groups released around 0.13 mg of Ca^{2+} to the incubation media and this value remained stable over the six weeks. In contrast, PLGA-containing CPCs showed a significantly higher calcium release ($p < 0.001$) at all time points and, therefore, a higher CPC matrix degradation. After 1 week of incubation PLGA-containing samples presented a similar calcium release to PLGA-free groups. After 2 weeks of incubation, on the other hand, PLGA-containing samples presented an eightfold increase. This difference augmented over time and reached a maximum Ca^{2+} release of around 11 mg, being the differences among PLGA-containing groups not significantly different ($p > 0.05$). Regarding sucrose release, after one week, all sucrose containing groups showed an initial release, which was maximal after approximately four weeks of degradation. It was observed that the maximum sucrose released matches the theoretical maximum release expected.

Morphology

SEM images were taken from all the samples at different incubation times to monitor the morphological appearance of the degradation process (Fig. 3). CPC samples did not show any morphological modification during degradation. On the other hand, sucrose porogens were observed in CPC/S20 and CPC/PLGA/S20 before degradation (week 0), while after 1 week of incubation no sucrose porogens but macropores were present instead. PLGA porogens were observed before incubation and at week 1 of incubation while at week 6 of incubation the PLGA was degraded.

Porosity evaluation

Total porosity of the different CPC samples was calculated by three different techniques; helium pycnometry was used to measure total porosity, mercury porosimetry was used to measure open porosity and microCT was used to measure macroporosity.

Prior to incubation of the different cement samples, helium pycnometry [Fig. 4(a)] showed that CPC samples presented the highest total porosity (48.0%) and the presence of sucrose and PLGA decreased the total porosity, being CPC/PLGA/S20 the group showing the lowest porosity (26.0%). After week 1, the total porosity increased up to 51.1% in sucrose-containing samples due to sucrose dissolution. The effect of PLGA degradation was only noticeable after 6 weeks of incubation, when total porosity increased significantly ($p < 0.01$) up to approximately 78%.

The results obtained by mercury porosimetry about the open porosity of the different samples can be observed in Figure 4(b). The different groups at both time points showed an open porosity with similar but lower values to those of the total porosity. At week 1, open porosity percentage in CPC was the lowest (35.7%). PLGA incorporation slightly increased the open porosity up to approximately 40–43% at week 1 and up to 73% at week 6. On the other hand, sucrose incorporation increased the open porosity at week 1 compared to CPC (up to 43.6% for CPC/ S20). At week 6, 20 wt % of sucrose only increased about 1% the open porosity compared to CPC or CPC/PLGA control groups. Macroporosity was measured by microCT [Fig. 4(c)]. Macroporosity of CPC was lower than 0.6% at all time points. Groups containing only sucrose (i.e., CPC/S10 and CPC/S20) showed a higher macroporosity ($p < 0.01$) that remained stable over time ($p > 0.05$). CPC/PLGA showed an initially low macroporosity (3.0%), which increased up to 17.5% after 6 weeks. CPC/PLGA/S10 and CPC/PLGA/S20 presented an initial macroporosity significantly higher than CPC/PLGA of 6.8% ($p < 0.05$) and 11.4% ($p < 0.01$), respectively. After 6 weeks, only CPC/PLGA/S20 presented a significantly higher macroporosity than CPC/PLGA ($p < 0.05$).

Figure 5(a) shows representative images of the microCT analysis before incubation and at 6 weeks of incubation. An obvious difference in grayscale appearance between cement samples with and without PLGA porogens was observed, with a decrease in gray values as a sign of CPC degradation. Figure 5(b) illustrates the increase in pore formation for a representative CPC/PLGA/S20 sample, where blue voxels represent the porosity created over incubation time.

Pore size distribution

Evaluation of pore size distribution was performed using microCT (Fig. 6). CPC samples presented a pore size distribution characterized by a main peak at about 60 μm, which was constant over time. Similarly, CPC/PLGA showed a main peak below 50 μm, which frequency gradually increased from week 0 to week 6. CPC/S10 and CPC/S20 showed a broader pore size distribution with pores ranging from 7 to 350 μm and an average pore size of 130 μm, which remained stable over time. On the other hand, the pore size distribution of CPC/PLGA/S10 and CPC/PLGA/S20 resembled the one of CPC/PLGA with a main peak below 50 μm, but larger pores were observed up to 450 μm for CPC/PLGA/S10 and up to

350 μm for CPC/PLGA/S20. Furthermore, the average pore size decreased over time, which resulted in a larger percentage of the pores being in the 0–50 μm range.

DISCUSSION

The aim of this study was to evaluate multimodal *in vitro* pore formation behavior and degradation of CPC upon incorporation of porogens with different modes of degradation; for this, we used water-soluble sucrose porogens, hydrolytically degrading PLGA porogens, and combinations thereof. We hypothesized that sucrose porogens would lead to rapid pore formation, while PLGA porogens would result in late pore formation and additional degradation of the ceramic CPC matrix. For this study, we selected two different weight ratios of sucrose porogens (10 and 20 wt %) and one weight ratio of PLGA porogens (40 wt %). The *in vitro* incubation experiments confirmed that with inclusion of sucrose porogens, CPC retains handling properties required for clinical application and that sucrose porogen incorporation into CPC results in rapid mass loss and pore formation.

Assessment of the handling properties of the CPC composites showed that the addition of sucrose increased the injectability, which represents a benefit for its clinical applicability. It is known that polysaccharides possess suitable rheological properties,[31,32] which might explain our observations on improved injectability of the sucrose-containing CPC pastes due to the dissolution of the sucrose already while mixing, which acts as a lubricant. On the other hand, the addition of PLGA did not significantly influence injectability in contrast to previous observations by others.[33] Unfortunately, the inclusion of sucrose also increased the final setting times to a large extent. The clinical meaning of final setting times is that, *in vivo*, the wound should be closed after that time. In our case, adding 20 wt % of sucrose resulted in final setting times beyond the clinically accepted window of 15–20 min, which might limit the *in vivo* use of the CPC/PLGA/sucrose to preset forms.[34–36] These results of setting time corroborate those of Smith et al.[25] who found that the addition of glucose porogens even had a worse effect on both initial (100 min) and final (250 min) setting times.

Mass loss of the CPC composites was monitored during 6 weeks. Already after one day, CPC/sucrose formulations showed a mass loss proportional to the initial amount of sucrose within the CPC, which hence directly relates to sucrose dissolution. In contrast, CPC/PLGA showed gradual mass loss occurring between week 1 and 4. For PLGA-containing CPC formulations, this mass loss coincided with a decrease in pH, which indicates a direct relation to the hydrolytic degradation of PLGA in its acidic degradation products lactic and glycolic acid.[18,37] As a result of pH decrease and the incubation system used in our experiments (that is, one cylindrical sample in 10 mL PBS at 37°C), the Ca^{2+} release reached approximately 15% of the total calcium present in the initial samples, indicating degradation of the CPC matrix starting at pH levels below 6 (after week 1). This acidification is more pronounced for *in vitro* studies, for which different volumes have been used (range: 1.5 mL–3 L), but which does not affect the *in vivo* bone formation process, likely due to the large buffer capacity of the human body.[16,21,38–41]

Regarding porosity analysis, helium pycnometry provided a clear overview of pore formation behavior within the different CPC formulations. Prior to the incubation of CPC

samples, when PLGA and sucrose porogens were still intact, the total porosity measured by this method corresponded to the intrinsic microporosity of the CPC, which typically varies between 30 and 50 vol % depending on the processing conditions (i.e., LPR) and ceramic component of the composition.[42] During incubation experiments, the increase in total porosity corresponded to sucrose porogen dissolution at an early stage and to CPC and PLGA degradation at a later stage. Takagi and Chow[23] introduced 25 wt % of sucrose particles into CPC and observed a microporosity of 31.4% and a total porosity of ~50%. Our results corroborate theirs with a microporosity of 38.4 and 33.8% in CPC/S10 and CPC/S20, respectively. Theoretically, comparing the total porosity of both groups, we can assume that every extra 10 wt % of sucrose decreases the microporosity with about 5%. Therefore, the inclusion of 25 wt % of sucrose would lead to a microporosity of 31.5%, which is what Takagi and Chow observed.

Mercury porosimetry showed that the total porosity was highly interconnected and open porosity ranged from 78% (for CPC samples at week 1, as a percentage of the total porosity) to 92% (for PLGA containing samples at week 6). The fact that the pores within our CPC formulations are highly interconnected represents an advantage toward their *in vivo* application, as open porosity facilitates fluid inflow and tissue ingrowth into the CPC matrix. MicroCT analysis showed that macroporosity was highly influenced by the presence of sucrose porogens at an initial stage and by PLGA porogens at a later stage. In line with our results, Smith et al.[25] previously observed a clear relation between the presence of the water-soluble porogen glucose and macroporosity at an early stage.

It is known that pore size is an important factor for bone regeneration. Therefore, pore size distributions were calculated. The pore size distribution for CPC and CPC/ PLGA were very similar from a pore size perspective, which is related to the similarity in size between air bubble-related pores created during CPC manufacturing and PLGA porogens (approximately 60 μm). In contrast, sucrose porogens induced a rather wide pore size distribution, with an average pore size of 100–150 μm and a maximum pore size of approximately 350 μm. In view of the average size of the sucrose porogens of 400 μm, this suggests that partial dissolution occurred in the time window from adding liquid component to the powder cement component till cement setting. Still, the obtained pore sizes with sucrose porogens correspond to pore sizes that are generally considered adequate for bone regeneration (100–600 μm).[43,44] Furthermore, the combination of PLGA porogens with sucrose porogens within CPC increased the average size of the formed pores, which likely facilitates early perfusion of CPC by body fluids and tissue ingrowth, and hence degradation of the ceramic CPC-matrix at a later stage, the latter further accelerated by the effect of acidic degradation products of the PLGA porogens.

The overall results obtained in the present study suggest that the combination of PLGA and sucrose porogens in CPCs have a potential for future clinical use. Furthermore, CPC/ PLGA formulations have been widely studied and, together with the fact that sucrose is considered a GRAS (i.e., generally regarded as safe) material, the here evaluated multimodal pore forming concept represents a straightforward approach for implementation in bone regenerative and augmentation procedures.

CONCLUSION

The current study evaluated the multimodal pore formation and degradation behavior of CPC upon the incorporation of a water-soluble and an acidifying hydrolytically degradable porogen. The incorporation of water soluble sucrose porogens into CPC largely retained the required handling properties. Sucrose porogen incorporation into CPC accelerated the mass loss proportional to the amount of sucrose added and created early stage macroporosity. The combination of sucrose porogens with PLGA porogens into CPC renders the CPC/porogen system into one that provides early stage macroporosity by rapid sucrose dissolution and late stage expansion of porosity and CPC degradation by hydrolytic degradation of PLGA into its acidic degradation products lactic and glycolic acid. Future studies should focus on evaluating the *in vivo* performance of CPC/PLGA/sucrose formulations.

Acknowledgments

Contract grant sponsor: Xunta de Galicia; contract grant number: ED481B 2017/063 (to L.D.-G.)

Contract grant sponsor: Life Science and Health, Dutch Ministry of Economic Affairs

Contract grant sponsor: Army, Navy, NIH, Air Force, VA and Health Affairs; contract grant number: W81XWH-14–2-0004

REFERENCES

1. Sanzana ES, Navarro M, Macule F, Suso S, Planell JA, Ginebra MP. Of the in vivo behavior of calcium phosphate cements and glasses as bone substitutes. Acta Biomater 2008;4:1924–1933. [PubMed: 18539102]
2. Nihouannen DL, Saffarzadeh A, Aguado E, Goyenvalle E, Gauthier O, Moreau F, Pilet P, Spaethe R, Daculsi G, Layrolle P. Osteogenic properties of calcium phosphate ceramics and fibrin glue based composites. J Mater Sci Mater Med 2007;18:225–235. [PubMed: 17323153]
3. Hannink G, Arts JJ. Bioresorbability, porosity and mechanical strength of bone substitutes: What is optimal for bone regeneration? Injury 2011;42:S22–S25.
4. del Real RP, Wolke JGC, Vallet-Regí M, Jansen JA. A new method to produce macropores in calcium phosphate cements. Biomaterials 2002;23:3673–3680. [PubMed: 12109693]
5. Ooms E, Wolke J, Van de Heuvel M, Jeschke B, Jansen J. Histological evaluation of the bone response to calcium phosphate cement implanted in cortical bone. Biomaterials 2003;24:989–1000. [PubMed: 12504521]
6. Frankenburg EP, Goldstein SA, Bauer TW, Harris SA, Poser RD. Biomechanical and histological evaluation of a calcium phosphate cement. J Bone Joint Surg Am 1998;80:1112–1124. [PubMed: 9730120]
7. Yuan H, Li Y, De Bruijn J, De Groot K, Zhang X. Tissue responses of calcium phosphate cement: A study in dogs. Biomaterials 2000; 21:1283–1290. [PubMed: 10811310]
8. Ginebra M, Fernandez E, De Maeyer E, Verbeeck R, Boltong M, Ginebra J, Driessens F, Planell J. Setting reaction and hardening of an apatitic calcium phosphate cement. J Dent Res 1997;76:905–912. [PubMed: 9126187]
9. Charrière E, Terrazzoni S, Pittet C, Mordasini P, Dutoit M, Lemaıtre J, Zysset P. Mechanical characterization of brushite and hydroxyapatite cements. Biomaterials 2001;22:2937–2945. [PubMed: 11561900]
10. Comuzzi L, Ooms E, Jansen JA Injectable calcium phosphate cement as a filler for bone defects around oral implants: An experimental study in goats. Clin Oral Implants Res 2002;13:304–311. [PubMed: 12010162]

11. Renno ACM, van de Watering FCJ, Nejadnik MR, Crovace MC, Zanotto ED, Wolke JGC, Jansen JA, van den Beucken JJJP. Incorporation of bioactive glass in calcium phosphate cement: An evaluation. Acta Biomater 2013;9:5728–5739. [PubMed: 23159565]
12. del Real RP, Ooms E, Wolke JG, Vallet-Regi M, Jansen JA In vivo bone response to porous calcium phosphate cement. J Biomed Mater Res A 2003;65:30–36. [PubMed: 12635151]
13. Kroese-Deutman HC, Ruhe PQ, Spauwen PH, Jansen JA. Bone inductive properties of rhBMP-2 loaded porous calcium phosphate cement implants inserted at an ectopic site in rabbits. Biomaterials 2005;26:1131–1138. [PubMed: 15451632]
14. Almirall A, Larrecq G, Delgado J, Martınez S, Planell J, Ginebra M. Fabrication of low temperature macroporous hydroxyapatite scaffolds by foaming and hydrolysis of an α-TCP paste. Biomaterials 2004;25:3671–3680. [PubMed: 15020142]
15. LeGeros RZ. Biodegradation and bioresorption of calcium phosphate ceramics. Clin Mater 1993;14:65–88. [PubMed: 10171998]
16. Félix Lanao RP, Leeuwenburgh SCG, Wolke JGC, Jansen JA. Bone response to fast-degrading, injectable calcium phosphate cements containing PLGA microparticles. Biomaterials 2011;32: 8839–8847. [PubMed: 21871661]
17. Schwach G, Oudry N, Delhomme S, Lück M, Lindner H, Gurny R. Biodegradable microparticles for sustained release of a new GnRH antagonist–part I: Screening commercial PLGA and formulation technologies. Eur J Pharm Biopharm 2003;56:327–336. [PubMed: 14602174]
18. Félix Lanao RP, Leeuwenburgh SCG, Wolke JGC, Jansen JA. In vitro degradation rate of apatitic calcium phosphate cement with incorporated PLGA microspheres. Acta Biomater 2011;7:3459–3468. [PubMed: 21689794]
19. Liao H, Felix Lanao RP, van den Beucken JJ, Zhou N, Both SK, Wolke JG, Jansen JA. Size matters: Effects of PLGA-microsphere size in injectable CPC/PLGA on bone formation. J Tissue Eng Regen Med 2016;10:669–678. [PubMed: 24170734]
20. Hoekstra JWM, Ma J, Plachokova AS, Bronkhorst EM, Bohner M, Pan J, Meijer GJ, Jansen JA, van den Beucken JJ. The in vivo performance of CaP/PLGA composites with varied PLGA microsphere sizes and inorganic compositions. Acta Biomater 2013;9: 7518–7526. [PubMed: 23511808]
21. Grosfeld EC, Hoekstra JW, Herber RP, Ulrich DJ, Jansen JA, van den Beucken JJ. Long-term biological performance of injectable and degradable calcium phosphate cement. Biomed Mater 2016; 12:015009. [PubMed: 27934787]
22. Yoshikawa T, Suwa Y, Ohgushi H, Tamai S, Ichijima K. Self-setting hydroxyapatite cement as a carrier for bone-forming cells. Biomed Mater Eng 1996;6:345–351. [PubMed: 8986355]
23. Takagi S, Chow LC. Formation of macropores in calcium phosphate cement implants. J Mater Sci Mater Med 2001;12:135–139. [PubMed: 15348319]
24. Xu HH, Quinn JB, Takagi S, Chow LC, Eichmiller FC. Strong and macroporous calcium phosphate cement: Effects of porosity and fiber reinforcement on mechanical properties. J Biomed Mater Res 2001;57:457–466. [PubMed: 11523041]
25. Smith BT, Santoro M, Grosfeld EC, Shah SR, van den Beucken JJ, Jansen JA, Mikos AG. Incorporation of fast dissolving glucose porogens into an injectable calcium phosphate cement for bone tissue engineering. Acta Biomater 2016;50:68–77. [PubMed: 27956363]
26. Barralet JE, Grover L, Gaunt T, Wright AJ, Gibson IR. Preparation of macroporous calcium phosphate cement tissue engineering scaffold. Biomaterials 2002;23:3063–3072. [PubMed: 12102177]
27. Qi X, Ye J. Mechanical and rheological properties and injectability of calcium phosphate cement containing poly (lactic-co-glycolic acid) microspheres. Mater Sci Eng C 2009;29:1901–1906.
28. Smith F, Gilles M, Hamilton J, Godees P. Colorimetric method for determination of sugar related substances. Anal Chem 1956;28: 350–356.
29. Hagenmüller H, Hofmann S, Kohler T, Merkle HP, Kaplan DL, Vunjak-Novakovic G, Müller R, Meinel L. Non-invasive time-lapsed monitoring and quantification of engineered bone-like tissue. Ann Biomed Eng 2007;35:1657–1667. [PubMed: 17546503]

30. Lambers FM, Kuhn G, Schulte FA, Koch K, Müller R. Longitudinal assessment of in vivo bone dynamics in a mouse tail model of postmenopausal osteoporosis. Calcif Tissue Int 2012;90:108–119. [PubMed: 22159822]

31. Andrianjatovo H, Lemaitre J. Effects of polysaccharides on the cement properties in the monocalcium phosphate/b-tricalcium phosphate system. Innov Technol Biol Med 1995;16:140–147.

32. Burguera EF, Xu HH, Weir MD. Injectable and rapid-setting calcium phosphate bone cement with dicalcium phosphate dihydrate. J Biomed Mater Res B 2006;77:126–134.

33. Habraken WJ, Wolke JG, Mikos AG, Jansen JA Injectable PLGA microsphere/calcium phosphate cements: Physical properties and degradation characteristics. J Biomater Sci Polym Ed 2006;17: 1057–1074. [PubMed: 17094642]

34. Khairoun I, Boltong M, Driessens F, Planell J. Effect of calcium carbonate on clinical compliance of apatitic calcium phosphate bone cement. J Biomed Mater Res A 1997;38:356–360.

35. Khairoun I, Boltong MG, Driessens FCM, Planell JA. Some factors controlling the injectability of calcium phosphate bone cements. J Mater Sci Mater Med 1998;9:425–428. [PubMed: 15348854]

36. Takagi S, Chow LC, Ishikawa K. Formation of hydroxyapatite in new calcium phosphate cements. Biomaterials 1998;19:1593–1599. [PubMed: 9830985]

37. Habraken W, Wolke J, Mikos A, Jansen J. PLGA microsphere/calcium phosphate cement composites for tissue engineering: In vitro release and degradation characteristics. J Biomater Sci Polym Ed 2008;19:1171–1188. [PubMed: 18727859]

38. Sariibrahimoglu K, An J, van Oirschot BA, Nijhuis AW, Eman RM, Alblas J, Wolke JG, van den Beucken JJ, Leeuwenburgh SC, Jansen JA. Tuning the degradation rate of calcium phosphate cements by incorporating mixtures of polylactic-co-glycolic acid microspheres and glucono-delta-lactone microparticles. Tissue Eng Part A 2014;20:2870–2882. [PubMed: 24819744]

39. Habraken WJ, Liao HB, Zhang Z, Wolke JG, Grijpma DW, Mikos AG, Feijen J, Jansen JA. In vivo degradation of calcium phosphate cement incorporated into biodegradable microspheres. Acta Biomater 2010;6:2200–2211. [PubMed: 20026289]

40. Krieger NS, Frick KK, Bushinsky DA. Mechanism of acid-induced bone resorption. Curr Opin Nephrol Hypertens 2004;13:423–436. [PubMed: 15199293]

41. Klijn RJ, van den Beucken JJ, Félix Lanao RP, Veldhuis G, Leeuwenburgh SC, Wolke JG, Meijer GJ, Jansen JA. Three different strategies to obtain porous calcium phosphate cements: Comparison of performance in a rat skull bone augmentation model. Tissue Eng Part A 2012;18:1171–1182. [PubMed: 22292519]

42. Ginebra MP, Traykova T, Planell JA. Calcium phosphate cements as bone drug delivery systems: A review. J Control Release 2006; 113:102–110. [PubMed: 16740332]

43. Hulbert S, Young F, Mathews R, Klawitter J, Talbert C, Stelling F. Potential of ceramic materials as permanently implantable skeletal prostheses. J Biomed Mater Res A 1970;4:433–456.

44. Simske SJ, Ayers RA, Bateman T. Porous Materials for Bone Engineering Zürich: Trans Tech Publications, Inc.; 1997 p 151–182.

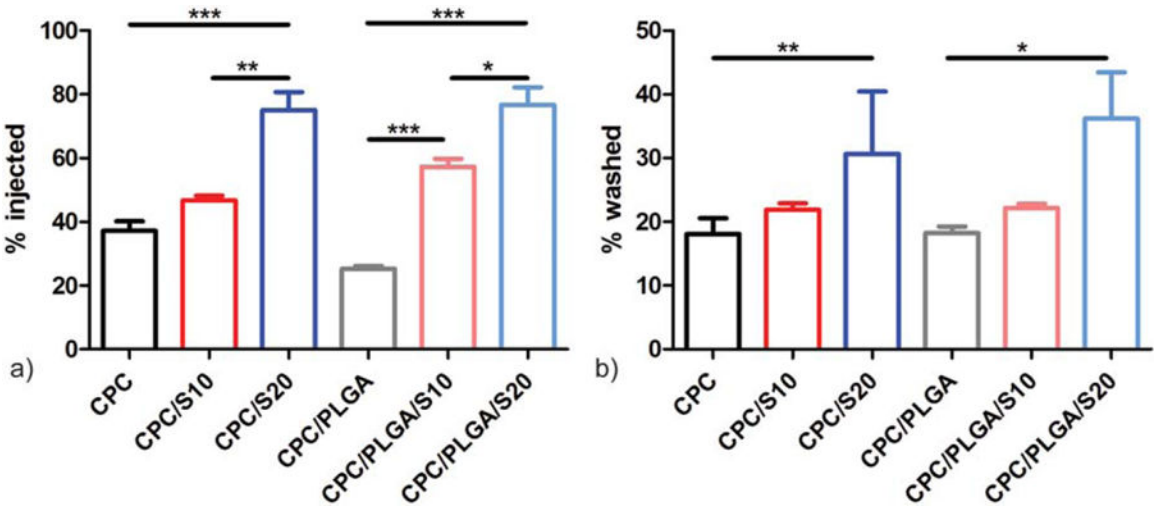

FIGURE 1.

Handling properties of CPC composites: (a) injectability % and (b) washout % of the different cement formulations ($n = 3$); *$p < 0.05$, **$p < 0.01$, and ***$p < 0.001$; error bars represent standard deviation (SD).

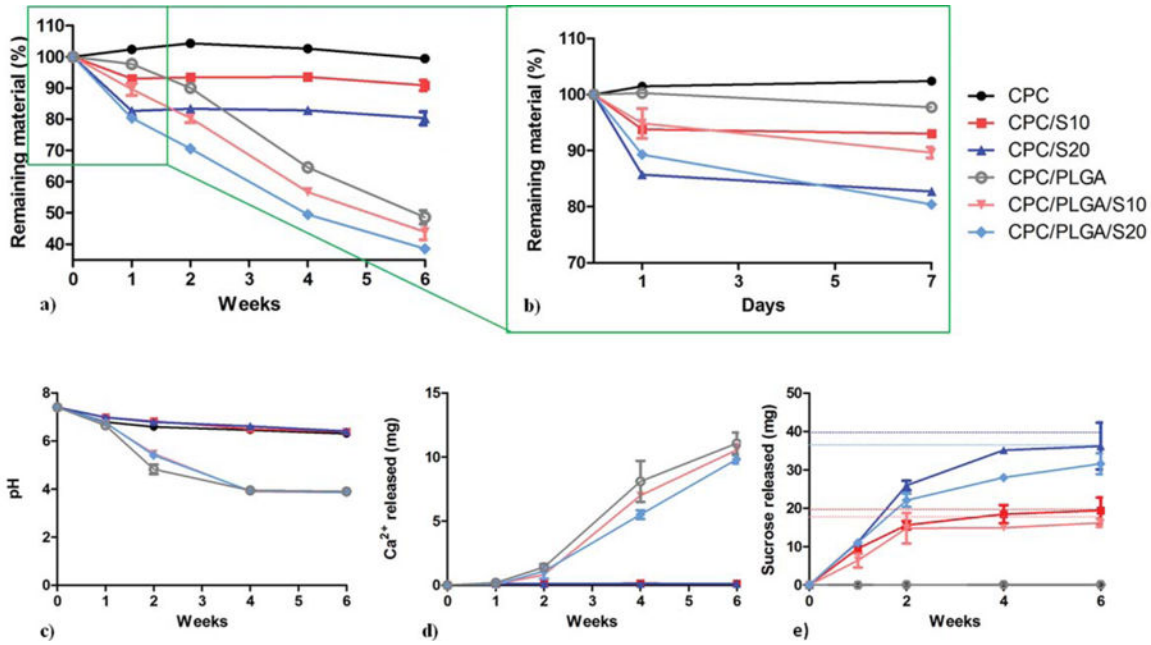

FIGURE 2.

Degradation of CPC composites. (a) Mass loss of each groups represented by the remaining material as a function of degradation time and (b) magnification of the mass loss in week 1. (c) pH, (d) cumulative calcium release and (e) cumulative sucrose release and maximum theoretical release of each cement formulation to the surrounding PBS. Error bars represent SD.

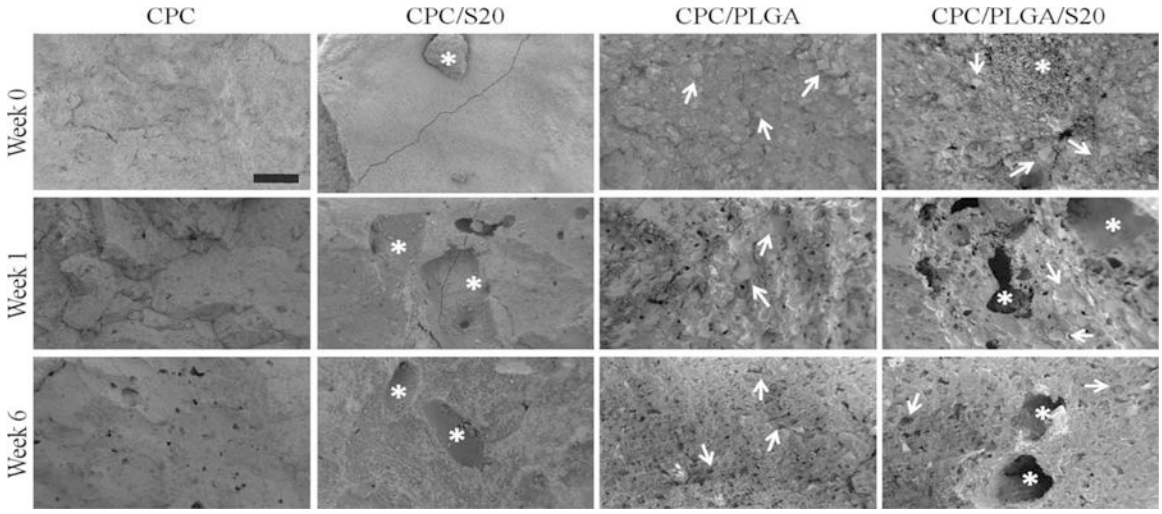

FIGURE 3.

Representative SEM images of CPC, CPC/S20, CPC/PLGA, and CPC/PLGA/S20 formulations before incubation (week 0), after 1 week incubation and after 6 weeks incubation. Black bar represents 200 μm. Long yellow arrows indicate either presence of sucrose or sucrose-related porosity. Short red arrows indicate either the presence of PLGA or PLGA-related porosity.

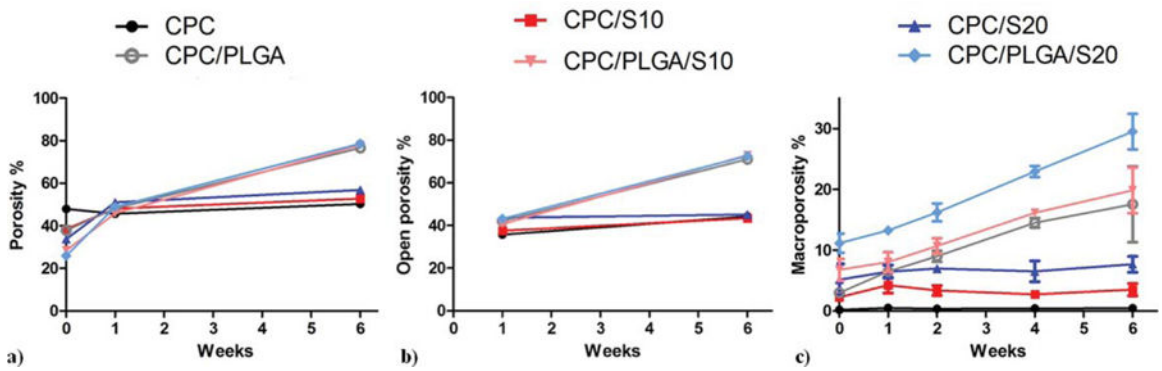

FIGURE 4.

Porosity of CPC composites measured by (a) helium pycnometry (total porosity), (b) mercury porosimetry (open porosity), and (c) microCT (macroporosity). Error bars represent SD.

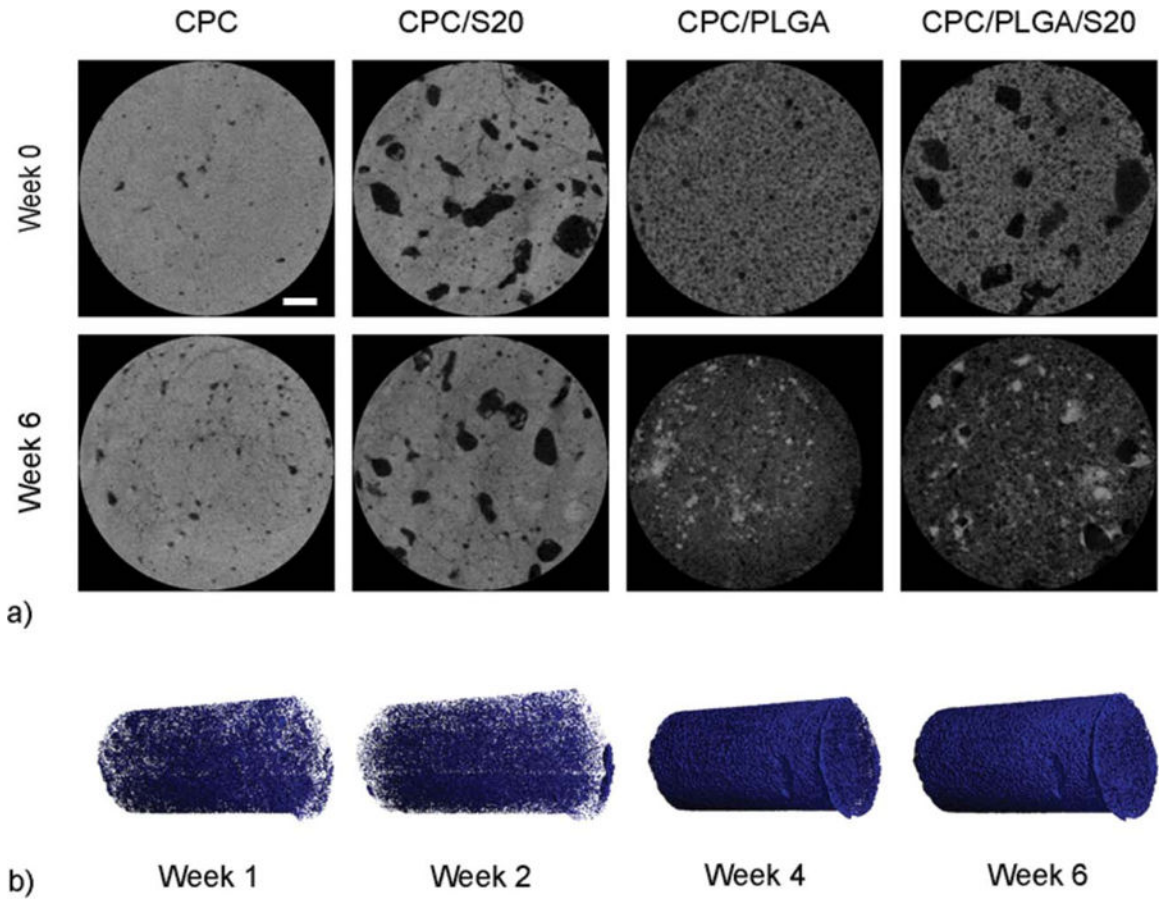

FIGURE 5.

(a) Representative microCT images of CPC, CPC/S20, CPC/PLGA, and CPC/PLGA/S20 formulations before incubation (week 0) and after 6 weeks incubation (white line represents 0.5 mm). (b) Three-dimensional reconstructed microCT of CPC/PLGA/S20, in which blue voxels represent pore formation within one sample over time.

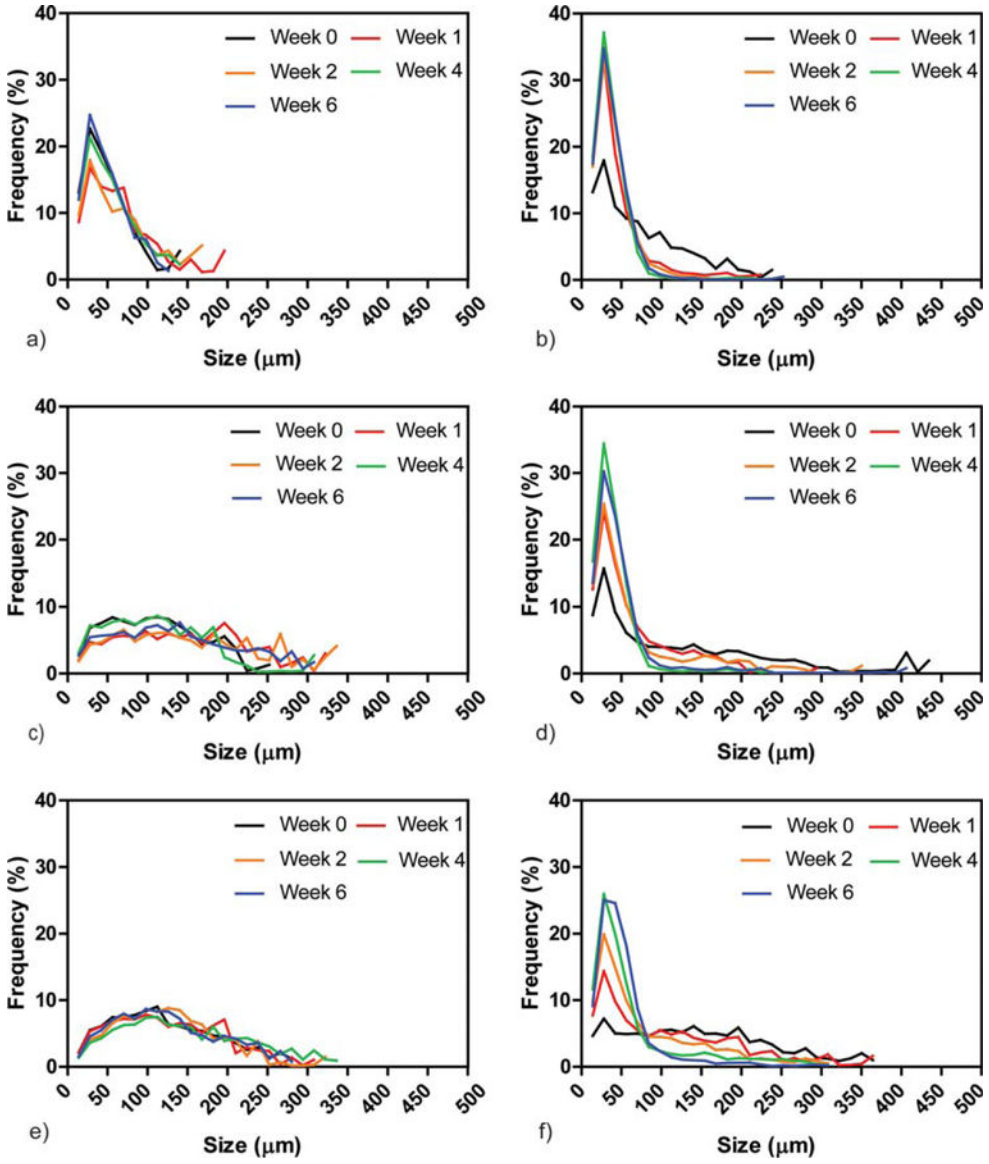

FIGURE 6.

Pore size distribution (μm) of (a) CPC, (b) CPC/PLGA, (c) CPC/S10, (d) CPC/PLGA/S10, (e) CPC/S20, and (f) CPC/PLGA/S20 composites at weeks 0, 1, 2, 4, and 6 of incubation.

TABLE I.

Abbreviations and Compositions of the Various CPC Formulations

Abbreviation	α-TCP[a] (wt %)	PLGA (wt %)	Sucrose (wt %)	LPR
CPC	100	0	0	0.47
CPC/S10	90	0	10	0.36
CPC/S20	80	0	20	0.3
CPC/PLGA	60	40	0	0.41
CPC/PLGA/S10	54	36	10	0.29
CPC/PLGA/S20	48	32	20	0.23

[a] α-TCP, alpha tricalcium phosphate; PLGA, poly(DL-lactic-*co*-glycolic acid); LPR, liquid-to-powder ratio.

TABLE II.

Setting Time of the Different Cement Formulations (n=3)

	Setting Time (min)	
CPC Formulation	**Initial**	**Final**
CPC	3.1 ± 0.1	7.4 ± 0.2
CPC/S10	3.5 ± 0.2	9.4 ± 0.7
CPC/S20	5.1 ± 0.5	36.3 ± 2.8
CPC/PLGA	3.4 ± 0.2	9.6 ± 0.9
CPC/PLGA/S10	4.1 ± 0.5	18.9 ± 1.2
CPC/PLGA/S20	9.1 ± 0.2	79.0 ± 3.0